2011 American Control Conference
on O'Farrell Street, San Francisco, CA, USA
June 29 - July 01, 2011

Long-Baseline Acoustic Localization of the *Seaglider* Underwater Glider

Laszlo Techy* Kristi A. Morgansen† and Craig A. Woolsey‡

Abstract— **This paper describes a long-baseline underwater acoustic localization system that was developed to provide three-dimensional position information for the *Seaglider* underwater vehicle. The accurate inertial position of the glider can be used to estimate performance characteristics and to validate novel motion control and path planning strategies in future experiments. The system consists of three acoustic transponders that are placed at known locations at the surface of the water. An extended Kalman filter with RTS smoothing was used to obtain filtered estimates of the states. The filtering methods have been tested both in simulations and in field experiments.**

I. Introduction

Buoyancy-driven underwater gliders are highly efficient marine vehicles that were originally developed to perform oceanographic data collection missions [2] [6]. Their flight characteristics depend on the amount of negative or positive net weight and on the location of movable internal masses. These vehicles are extremely efficient because they spend most of their time in a steady, trim flight condition, where they do not actively expend energy. Apart from the occasional sensor measurements and automatic scheduled self-tests, they only use energy when they change their trim flight condition, such as transitioning from steady descent to ascent, or rolling to one side in order to turn. Since much of the energy used is expended during these trim adjustments, significant energy savings are anticipated by the use of efficient maneuvering strategies that help achieve these desired flight conditions faster and with less control effort [9].

Recently developed efficient motion planning algorithms (see [7] [8] [11]) remain to be validated in underwater glider experiments. The focus of the research presented here was to devise a set of field experiments and develop the corresponding field equipment and data processing tools to be able to validate underwater glider motion control algorithms. The paper gives an overview of our initial results focused on developing a long-baseline (LBL) positioning system to track the path of the *Seaglider* underwater glider with high accuracy. The precise knowledge of the vehicle position during a dive enables computation of the vehicle speed, flight path angle and turning rate. LBL systems have been successfully used in the past for autonomous underwater vehicle (AUV) localization. The system described here is a type of moving LBL system (MLBL), in which the nodes are not stationary, but are equipped with navigation instruments (GPS), and act as moving reference beacons. The positioning system relies on acoustic round-trip travel time measurements that are processed by an extended Kalman filter (EKF). The EKF has the ability to incorporate the dynamic motion of the glider into the estimation algorithm, improving the estimation accuracy over that of less sophisticated geometric positioning methods. EKFs have been used in the past to estimate AUV positions and the magnitude of prevailing currents (see e.g. [5]). If data are available for post-processing, further improvements can be achieved by using smoothing algorithms. In this work a hybrid nonlinear RTS smoother has been implemented and its effectiveness verified in both simulations and experiments. These well-established algorithms proved very effective for precise underwater localization of the *Seaglider* AUV in a challenging shallow environment featuring multipath sources and strong tidal currents.

II. Background

A. Seaglider

The *Seaglider* is a long-range, long-endurance underwater glider that was developed at University of Washington as a collaboration between the Applied Physics Lab and the School of Oceanography [2]. The vehicle is equipped with conductivity-temperature-depth (CTD) sensors and optional additional scientific sensors, such as dissolved oxygen or optical backscatter. Other than science sensors, it also carries various navigation instruments, including: 1) a GPS unit to obtain a position fix when it surfaces, 2) a 3D compass to measure heading and tilt angle, and 3) an acoustic pinger/altimeter to obtain bottom depth and to be able to respond to acoustic interrogations in the low-frequency band (7-15 kHz).

*Research Associate, Department of Aeronautics and Astronautics, University of Washington, techy@u.washington.edu, IEEE Member.

‡Associate Professor, Department of Aeronautics and Astronautics, University of Washington, morgansen@aa.washington.edu, IEEE Senior Member.

†Associate Professor, Department of Aerospace and Ocean Engineering, Virginia Tech, cwoolsey@vt.edu, IEEE Senior Member.

B. Underwater Acoustic Ranging

In underwater applications, acoustic signals are primarily used for communication rather than radio signals due to poor propagation characteristics of radio signals in water [12]. The measured round-trip travel time of an acoustic signal is given by the equation

$$t_{RTT} = t_{TAT} + \frac{2R^{3D}}{c} + \epsilon, \tag{1}$$

where t_{TAT} is the turn-around time (the amount of time the electronics needs to detect the signal and send a response), R^{3D} is the slant range to the vehicle, and c is the speed of sound in water. The term ϵ represents the error between the true and measured round-trip travel time. Since the amount of error in the slant range measurements has a profound effect on the positioning accuracy, the sources of the errors need to be well understood.

Since the *Seaglider* provides temperature, salinity and depth information during its dive, the sound velocity profile can be calculated explicitly to minimize the scale factor error in the measurement equation (1) (see [10] or [12] for a survey). The variations in speed of sound at our test-site were minimal due to shallow operating depths and relatively minor salinity and temperature changes. We used the depth-averaged velocity profile in the calculations. (We note that the water in Port Susan exhibits strong salinity stratification due to the large amounts of freshwater entering the bay, creating a freshwater lens at the top of the water column. We excluded the top 20 m from our data processing due to poor acoustic returns in that region.)

Outliers often appear in the ranging solution due to multipath errors [13]. Reference [17] presents methods to remove outliers using spatial and temporal plausibility tests. Outliers in our ranging solution were infrequent and mostly isolated; we had success with a simple difference filter relying on temporal plausibility validation.

The error term in equation (1) can be written as the sum of two components: $\epsilon = \epsilon_s + v$, where ϵ_s represents the systematic errors, and v is the random noise component. After elimination of the major systematic error components, one is left with random measurement noise, which is primarily attributed to the residual timing errors in the signal processing. The probability distribution of the slant range (R^{3D}) measurement errors was estimated experimentally by building a sample relative likelihood histogram. The variance was found to be $\sigma_R^2 = 1.023\ \mathrm{m}^2$, with the distribution closely approximating a Gaussian distribution. Similarly, the variance of the compass measurement error was estimated experimentally as $\sigma_\psi^2 = 7.6 \cdot 10^{-5}\ \mathrm{rad}^2$.

C. LBL System Overview

The precise underwater location of the *Seaglider* may be found using a long-baseline (LBL) acoustic localization system. LBL systems are composed of several beacons in a network. The acoustic travel times between these beacons and the glider can be used to calculate the distance to each of the beacons. If the locations of the beacons are known, then the spatial position of the glider can be calculated using a suitable geometric algorithm (static position estimation) or a Kalman filter (dynamic position estimation).

The LBL system developed as part of this work consists of three identical nodes that are placed at known locations on the surface of the water. The nodes are placed on flotation devices to keep them above the water surface. To prevent them from drifting away from their deployment locations, they are anchored to the sea-floor. Each of the nodes consists of an acoustic ranging unit, a GPS antenna, a computer to synchronize the ranging measurements and to log data, and batteries to power all the components. All the electronics are housed inside Pelican case enclosures that were fitted with waterproof connectors for communication between the components. The measurement times were synchronized using GPS time so that only one transponder would ping at a time.

III. Position Estimation

Given an initial guess, the glider's position can be found using an iterative nonlinear least-squares algorithm

$$\boldsymbol{\theta} = (\boldsymbol{H}^T \boldsymbol{V}^{-1} \boldsymbol{H})^{-1} \boldsymbol{H}^T \boldsymbol{V}^{-1} \boldsymbol{r},$$

where $\boldsymbol{\theta}$ is the vector of estimated position correction, $\boldsymbol{V}$ is the measurement covariance matrix, $\boldsymbol{H}$ is the Jacobian matrix of the measurement equations, and $\boldsymbol{r}$ is the vector composed of the range measurements. Position estimates obtained this way will be referred to as "LS estimates."

The estimation accuracy can be significantly improved by using knowledge of the underlying vehicle dynamics and employing a dynamic filter. We used the commonly employed navigation equations extended with trivial dynamics for the velocities to allow the filter to adaptively estimate these unknown parameters:

$$\begin{aligned}
\dot{x}_N(t) &= V_a \cos\psi(t) + V_x && (2)\\
\dot{y}_E(t) &= V_a \sin\psi(t) + V_y && (3)\\
\dot{\psi}(t) &= u(t) && (4)\\
\dot{V}_a &= 0 && (5)\\
\dot{V}_x &= 0 && (6)\\
\dot{V}_y &= 0. && (7)
\end{aligned}$$

In the above equations $(x_N, y_E)^T$ are the planar position coordinates, V_a is the flow-relative speed of the glider,

V_x and V_y are the North and East components of the current velocity vector, $\psi(t)$ is the heading angle measured from North, and $u(t)$ is the turn rate of the vehicle, the only external input in this model. The turn rate is determined by the vehicle roll angle – information that can be obtained from the glider log files during post-processing. Notice that the velocities V_a, V_x and V_y are treated as states in the model with trivial dynamics. In reality they are unknown parameters, assumed to be constant or slowly varying, the values of which are to be estimated. Define the state vector as $\boldsymbol{x} = (x_N, y_E, \psi, V_a, V_x, V_y)^T$. Then equations (2)-(7) take the form $\dot{\boldsymbol{x}} = \boldsymbol{f}(\boldsymbol{x}, u) + \boldsymbol{w}$, where $\boldsymbol{w} \sim \mathcal{N}(\boldsymbol{0}, \boldsymbol{W})$ is the process noise, which is assumed to be zero-mean, Gaussian and white. At discrete time intervals, $t = kT$, measurements are available as defined by the output equations $\boldsymbol{y}(kT) = \boldsymbol{h}(\boldsymbol{x}(kT)) + \boldsymbol{v}(kT)$, where T is the sampling period, $k \in \mathbb{Z}$ and $\boldsymbol{v}(kT) \sim \mathcal{N}(\boldsymbol{0}, \boldsymbol{V})$ is the measurement noise which is also assumed to be zero-mean, Gaussian and white. The measurement vector for the underwater localization problem is

$$\boldsymbol{y}(kT) = \begin{pmatrix} R(kT) \\ \psi(kT) \end{pmatrix}, \tag{8}$$

where $R(kT)$ is the in-plane range measurement from a corresponding node, and $\psi(kT)$ is the vehicle heading angle obtained from the compass. Due to the uncertainties, the state of the dynamic system is a random process, and the best one can hope is to obtain its expected value $\hat{\boldsymbol{x}}$ and covariance matrix $\boldsymbol{P}$. The EKF gives these estimates, and under certain assumptions also guarantees that the solution is asymptotically optimal in the sense that the estimate is unbiased and of minimal variance. We used the EKF to estimate the states of the above dynamic system. Since the full data set was available for post-processing, we used the RTS smoothing method to improve the estimation accuracy of the filter (EKF + RTS). References [1] and [14] both provide a thorough treatment on batch state estimation algorithms. These methods are considered classical tools in the literature, and we will omit the corresponding equations. A comprehensive account including the specific equations is given in [15].

IV. Simulation Results

The flight of an underwater vehicle described by equations (2)-(7) was simulated on a computer. The constant glider velocity and current velocity components in the simulations were $V_a = 0.3$ m/s, $V_x = 0.1$ m/s, $V_y = -0.2$ m/s. These values were not known *a priori* to the algorithm; instead they were estimated by the EKF. The initial values for the filter were selected as $\hat{V}_{a_0} = 0.2$ m/s, $\hat{V}_{x_0} = 0$ m/s, $\hat{V}_{y_0} = 0$ m/s. During the simulations, a constant turn rate was used: $u = 0.9°/\text{s}$.

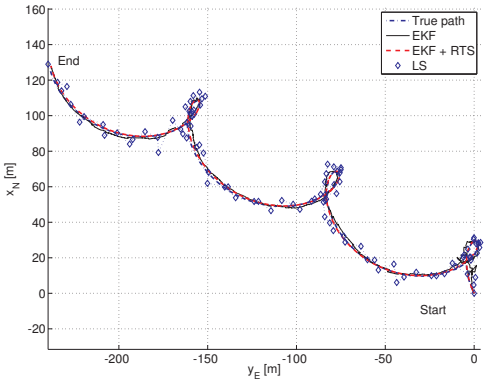

(a) Full data set.

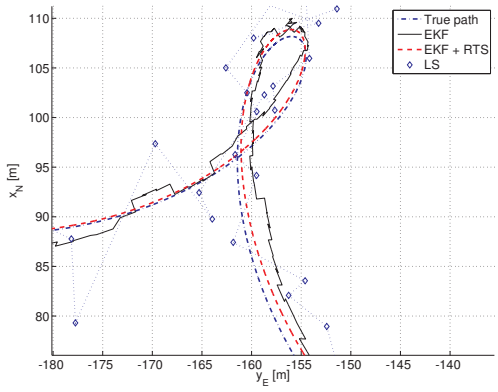

(b) Close-up version of Figure 1a.

Fig. 1: Planar position of the glider in simulations. The plots show the improved performance of the EKF + RTS filter. Figure 1b is a close-up version of Figure 1a.

The turn rate of the vehicle was not known for the estimator, so $u_{\text{model}} = 0$ was selected in the estimator equations. The process and measurement noise covariances were selected as $\boldsymbol{W} = 10^{-5}\text{diag}(0, 0, 7.6, 0.1, 0.1, 0.1)$, and $\boldsymbol{V} = \text{diag}(10\sigma_R^2, \sigma_\psi^2)$. The noise variance for the range measurement was selected an order of magnitude larger than the value estimated during calibration to simulate a worst-case scenario.

In the derivation of the Kalman filter, the process noise is assumed to be zero-mean and white, which is rarely the case in practice. Nevertheless, the Kalman filter exhibits a certain amount of robustness in erroneous selection of the process covariance matrix. For this reason the introduction of fictitious process noise in the Kalman filter equations has become common practice as a tuning method for the filter. Formally justified in [14], large process noise results in a filter that trusts the measurements more, and assumes that the model is incorrect or heavily corrupted with noise. Small process noise results in a filter that trusts the underlying model

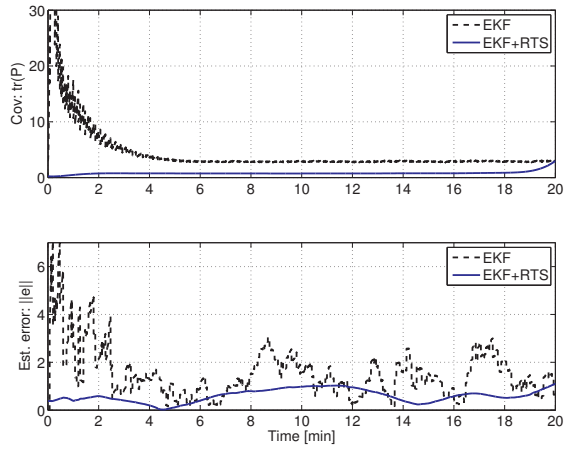

Fig. 2: Trace of the covariance matrix (top) and magnitude of the planar position error (bottom) in simulations for the EKF and the EKF+RTS filters.

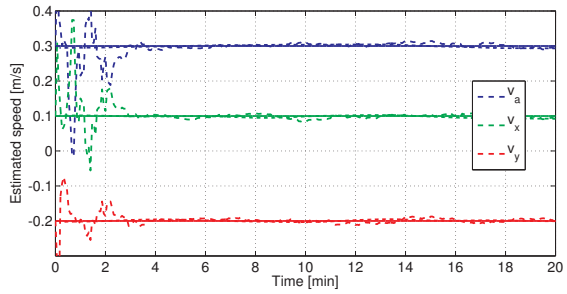

Fig. 3: Current speed components and glider flow-relative speed in simulations. Solid lines are true (constant) values; dashed lines are the EKF estimates; dashed-dotted lines are the EKF+RTS smoothing estimates (nearly identical to the true values).

more, yielding smoother paths in navigation problems, such as the one discussed in this paper.

Equations (2)-(3) represent simple translational kinematics and are assumed to be true and noise-free. The corresponding variances are hence zero. The turn rate dynamics are determined by the vehicle bank angle, which can be obtained from the glider log files in experiments. Since the turning rate was assumed noisy, a relatively large weight was selected for the corresponding entry in the process noise covariance matrix, $\boldsymbol{W}$. Most of the uncertainty in the system comes in the estimated current velocity components. Their values are initially assumed to be zero; in practice they may be spatially and temporally varying. The corresponding values in the covariance matrix were selected by considering the trade-off in convergence time versus the stability in the estimate. Smaller values tend to yield smoother convergence at a slower rate. If it is known that the glider flow-relative speed does not vary much during a dive and a close initial guess for the speed is available, then the corresponding weight may be selected smaller than for the other velocity components.

The simulation time was 20 minutes. A new measurement was obtained every 4 seconds: yielding a total of 300 consecutive range measurements. Three ranging node locations were selected in a triangle pattern, each approximately 1 km distance away from the origin where the simulation was started. The ranging measurements were obtained from the nodes one at a time in a round-robin fashion: each individual node providing an updated range every 12 seconds. In these simulations the compass was also sampled every 4 seconds. The simulation time-step for simulating the motion of the vehicle between measurements was 50 ms. After every third range measurement a static position estimate was also obtained using a simple spherical localization algorithm based on the iterative nonlinear least-squares method.

Parallel to the true vehicle model, an EKF estimator was also simulated. The measurements were obtained from the true model output with the addition of normally distributed measurement noise $\boldsymbol{v} \sim \mathcal{N}(\boldsymbol{0}, \boldsymbol{V})$. The EKF estimates were then used to calculate the RTS smoothed estimate (EKF + RTS).

Figures 1 - 3 show the results of these simulations. Planar plots of the glider position can be seen in Figure 1. As expected, the EKF estimates provide significant improvement over the static nonlinear least-squares based estimation algorithm. The dynamic filter produces estimates that take into account the dynamics of the underlying physical system. Furthermore, the EKF with RTS smoothing provides even greater improvement in the state estimates, as it uses all the measurements over the entire sampling interval including past and future times. Figure 2 shows the trace of the covariance matrix and the estimation error measured by $||\boldsymbol{e}|| = ||\boldsymbol{x} - \hat{\boldsymbol{x}}||$. The convergence of the estimated speed components is shown in Figure 3.

V. Experimental Results

The underwater localization methods described in Section III were used to estimate the underwater position of the *Seaglider* from experimental data collected in Port Susan on July 15, 2010. The simulation environment of Section IV was selected to be as representative of a typical experiment as possible. The same filter parameters were used for the experimental data processing that were identified to give good estimation results in simulations.

The results from dive number 18 can be seen in Figures 4-6. The dive started at 11:56 a.m. PDT, and lasted approximately 50 minutes. The data were reduced to include only the 30 minute portion that the glider

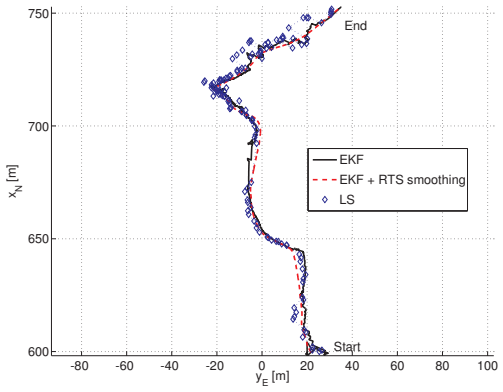

(a) Full data set.

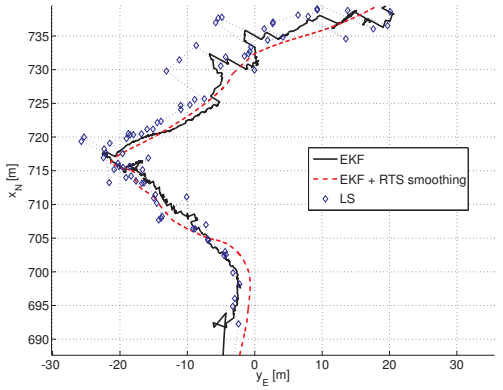

(b) Close-up showing smoothness of the estimated position.

Fig. 4: Underwater localization experimental results from July 15, 2010. The plots show planar position estimates for dive number 18 of the *Seaglider*.

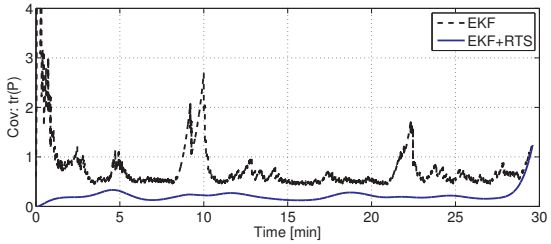

Fig. 5: Experimental results from July 15, 2010. The plots show the trace of the state covariance matrix $\boldsymbol{P}$.

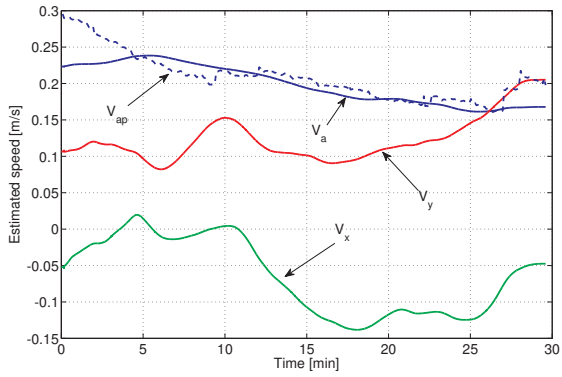

Fig. 6: Experimental results from July 15, 2010. Shown are the current velocity components (V_x,V_y) and the estimated flow-relative speed (V_a). The plot also shows the estimated flow-relative speed obtained from independent performance calculations: V_{ap} [2].

spent below 20 m depth, due to deterioration of acoustic responses near the water surface, as mentioned in Section II-B. Figures 4a-4b show the planar coordinates of the glider estimated position. The blue diamonds indicate the estimates obtained with the LS algorithm.

The trace of the covariance matrix of the state estimates, $\mathrm{tr}(\boldsymbol{P})$, can be seen in Figure 5. The major contributors of $\mathrm{tr}(\boldsymbol{P})$ are the spatial position variances. From the plot it is seen that the estimation accuracy is on the order of 30 cm and the filter converges to this value after three minutes into the experiment. The estimation covariance increases temporarily between 8 and 10 minutes. This corresponds to the point where the glider transitions from steady descent to ascent at the bottom of the dive. During this maneuver the glider is relatively close to the ocean bottom and the obtained responses suffer from multipath. The RTS smoothing algorithm appears to provide significant improvement in terms of the position estimation accuracy, measured by the magnitude of the estimation covariance matrix.

Figure 6 shows the estimates of the glider speed and the current velocity components. Low tide occurred in Port Susan at 2:07 p.m. on July 15, 2010: over two hours after the beginning of dive number 18. The current velocity estimates in Figure 6 indicate mostly East-Southeast current direction, which is in agreement with the expected tidal motion at that time. Figure 6 also shows the estimated flow-relative glider speed obtained from independent performance calculations. The performance calculations use the vehicle vertical descent rate, the pitch angle, and the vehicle hydrodynamic parameters to calculate the glide path angle and vehicle speed as described in [2]. There is good agreement between the two independent speed calculations.

We have deferred the discussion of observability until this point. The dynamic model (2)-(7) involves the adaptive estimation of both the current velocities and the vehicle's flow-relative velocity, which clearly raises observability concerns. The interested reader may find relevant information on this topic in [4] and [3]. The simulations confirmed that, as long as the system is

persistently excited, the EKF will converge if the ocean currents are constant or at most slowly varying. Such persistent excitation is achieved by having the vehicle travel along a curved pattern such as the one shown in Figure 1, as opposed to traveling along a straight line. Given that the currents identified by the EKF show significant variability, it is difficult to assess how accurate the current estimates identified during the field experiments truly are. The accuracy could be assessed by obtaining an independent measurement with Acoustic Doppler Current Profiler (ADCP) instrument, or by comparing the estimates to the output of computational ocean models for the given day and time. No ADCP instrument was at our disposal during the field experiments, and the comparison with the output of the Puget Sound Princeton Ocean Model (PSPOM) for July 15, 2010 did not yield satisfactory result.

Finally, we remark that the current estimation accuracy could be further improved if precise knowledge of the glider's flow-relative velocity, V_{ap}, is available. The flow-relative speed could be obtained from performance calculations as outlined in [2]. Such performance calculations presume accurate knowledge of the vehicle hydrodynamic parameters, which can be obtained from wind tunnel studies [16].

VI. Conclusions and Future Work

In this paper we described experimental underwater acoustic localization results that were performed with the *Seaglider* underwater glider in Port Susan in July 2010. An extended Kalman filter was used for dynamic parameter estimation and localization. The filter provides significant improvement over static estimation methods that do not consider the motion of the vehicle and only use present measurements to calculate the position. The accuracy can be further improved by employing an RTS smoother. The method provides smooth vehicle trajectories and significant error reduction confirmed by simulations and field experiments.

In our future work we will use the tools described in the paper in controlled glider experiments, to obtain a lookup table of flight parameters as a function of control actuator inputs. The localization system will be used to validate the efficiency of novel motion control algorithms.

Acknowledgements

The authors thank Fritz Stahr and Charlie Eriksen for their insight regarding Seaglider operations and oceanographic data collection. The authors thank undergraduate students Jake Quenzer, Ryan Tomokiyo, Tyler Beauchamp and Sami Kunze for their help with the field experiments. This work was sponsored by the Office of Naval Research under Grants No. N00014-10-1-0022 and No. N00014-08-1-0012.

References

[1] J. L. Crassidis and J. L. Junkins. *Optimal Estimation of Dynamic Systems*. Chapman & Hall/CRC, 2004.

[2] C. C. Eriksen, T. J. Osse, R. D. Light, T. Wen, T. W. Lehman, P. L. Sabin, J. W. Ballard, and A. M. Chiodi. Seaglider: A long-range autonomous underwater vehicle for oceanographic research. *Journal of Oceanic Engineering*, 26(4):424–436, 2001.

[3] M. F. Fallon, G. Papadopoulos, J.J. Leonard, and N.M. Patrikalakis. Cooperative AUV navigation using a single maneuvering surface craft. *The International Journal of Robotics Research*, 29(12):1461–1474, Sep. 2010.

[4] A. Gadre. *Observability analysis in navigation systems with an underwater vehicle application*. PhD thesis, Virginia Tech, Blacksburg, VA, January 2007.

[5] A.S. Gadre and D.J. Stilwell. A complete solution to underwater navigation in the presence of unknown currents based on range measurements from a single location. In *IEEE IROS 2005*, pages 1420 – 1425, aug. 2005.

[6] S. A. Jenkins, D. E. Humphreys, J. Sherman, J. Osse, C. Jones, N. Leonard, J. Graver, R. Bachmayer, T. Clem, P. Carroll, P. Davis, J. Berry, P. Worley, and J. Wasyl. Underwater glider system study. Technical Report 53, Scripps Institution of Oceanography, May 2003.

[7] R. Kraus, E. M. Cliff, and C. A. Woolsey. Optimal underwater glider trajectories in depth-varying currents. In *International Symposium on Unmanned Untethered Submersible Technology (UUST)*, Durham, NH, August 2009.

[8] R. Kraus, E. M. Cliff, C. A. Woolsey, and J. Luby. Optimal control of an undersea glider in a symmetric pull-up. In *International Symposium on Mathematical Theory of Networks and Systems (MTNS)*, Blacksburg, VA, August 2008.

[9] N. E. Leonard and J. G. Graver. Model-based feedback control of autonomous underwater gliders. *Journal of Oceanic Engineering*, 26(4):633–645, 2001.

[10] K. V. Mackenzie. Nine-term equation for sound speed in the oceans. *Journal of the Acoustical Society of America*, 70(3):807–812, 1981.

[11] N. Mahmoudian, J. Geisbert, and C. Woolsey. Approximate analytical turning conditions for underwater gliders: Implications for motion control and path planning. In *IEEE Journal of Oceanic Engineering*, volume 35, pages 131–143, January 2010.

[12] P. H. Milne. *Underwater Acoustic Positioning Systems*. Gulf Publishing Company, 1983. Chapter 2.

[13] E. Olson, J. J. Leonard, and S. Teller. Robust range-only beacon localization. *Journal of Oceanic Engineering*, 31(4):949 –958, oct. 2006.

[14] D. Simon. *Optimal State Estimation*. Wiley-Interscience, A John Wiley & Sons, Inc., Publication, 2006.

[15] L. Techy, K. A. Morgansen, and C. A. Woolsey. Long-Baseline Ranging System for Acoustic Underwater Localization of the Seaglider Underwater Glider. Technical report, University of Washington, Aeronautics & Astronautics, Seattle, WA, September 2010.

[16] L. Techy, R. Tomokiyo, J. Quenzer, T. Beauchamp, and K. A. Morgansen. Full-Scale Wind Tunnel Study of the Seaglider Underwater Glider. Technical report, University of Washington, Aeronautics & Astronautics, Seattle, WA, September 2010.

[17] J. Vaganay, J.J. Leonard, and J.G. Bellingham. Outlier rejection for autonomous acoustic navigation. In *Robotics and Automation, 1996. Proceedings., 1996 IEEE International Conference on*, volume 3, pages 2174–2181 vol.3, April 1996.